

Stabilizing lattice oxygen and interface chemistry of Ni-rich and Co-poor cathodes for high-energy lithium-ion batteries

Wu Wei^{a,#}, Zhihong Wang^{a,#}, Liyun Yao^a, Hao Jiang^{a,b*}, Chunzhong Li^{a,b}

^a Key Laboratory for Ultrafine Materials of Ministry of Education, School of Materials Science and Engineering, East China University of Science and Technology, Shanghai, 200237, China

^b Shanghai Engineering Research Center of Hierarchical Nanomaterials, School of Chemical Engineering, East China University of Science and Technology, Shanghai, 200237, China

These authors contributed equally to this work.

* Correspondence authors.

E-mail: jianghao@ecust.edu.cn

Part 1 Supporting Figures

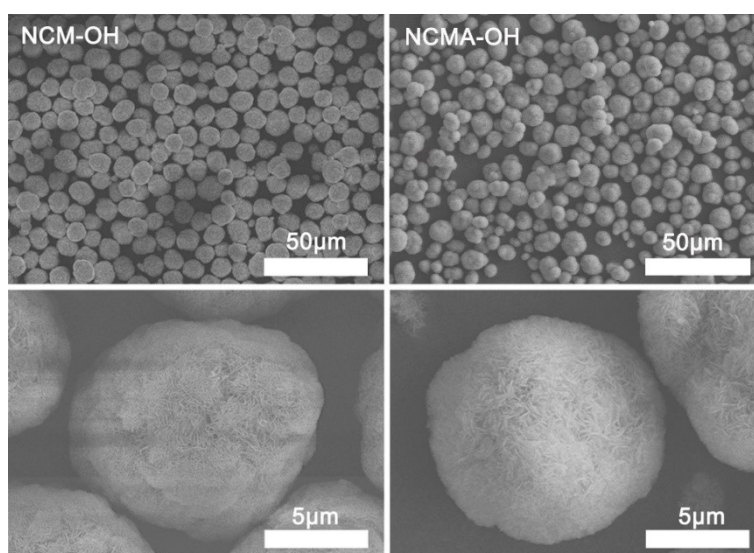


Figure S1 The SEM images of precursors for NCM and NCMA.

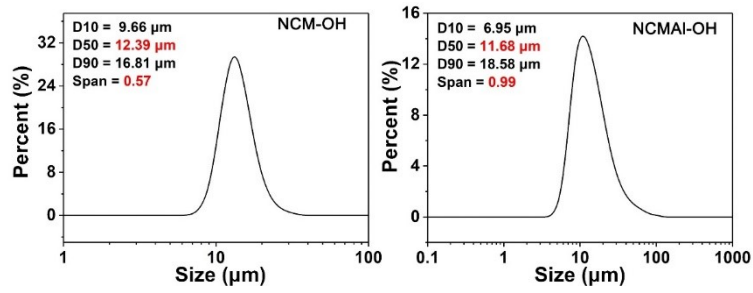


Figure S2 Particles size distribution of precursors for NCM and NCMA.

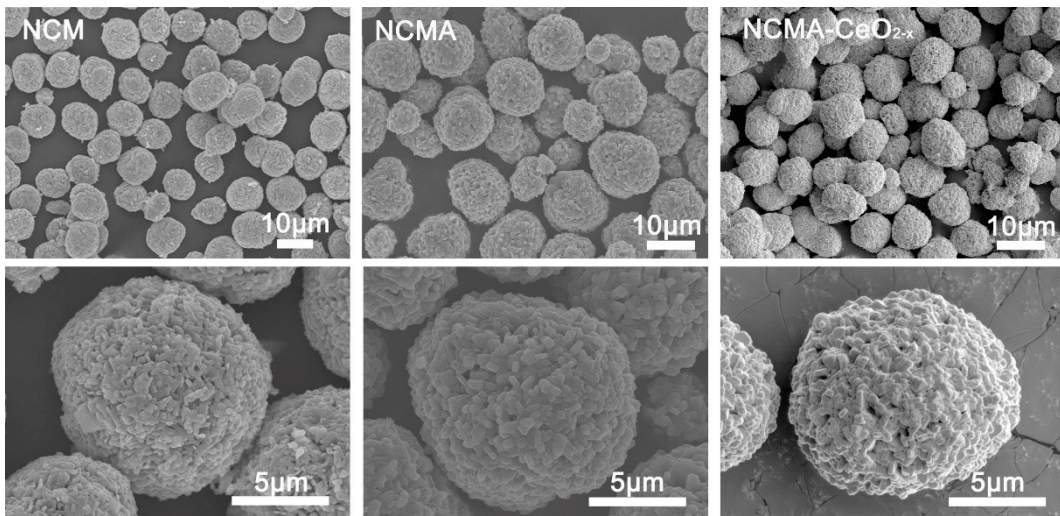


Figure S3 SEM images of NCM, NCMA, and NCMA-CeO_{2-x}.

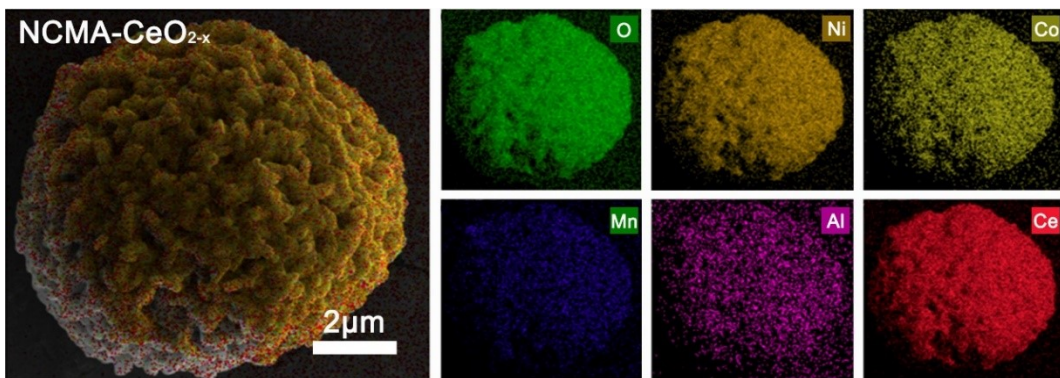


Figure S4 SEM image and the corresponding EDS mapping for NCMA-CeO_{2-x}.

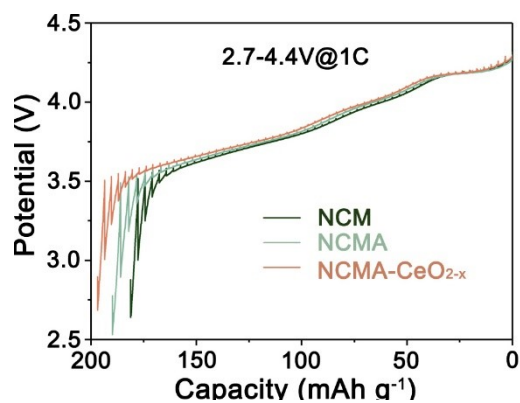


Figure S5 Discharge curves of GITT test.

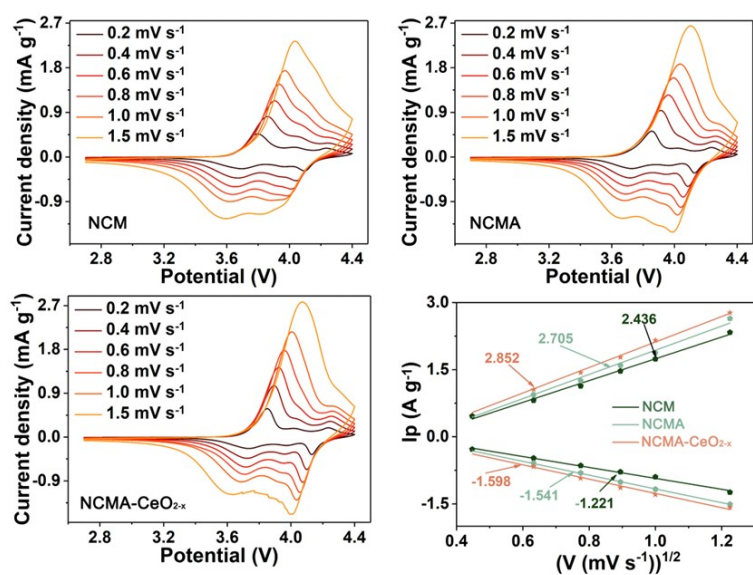


Figure S6 The CV curves from 0.2 to 1.5 mV s^{-1} and linear relationship between the anodic/cathodic peak current (i_p) and the square root of the scan rate ($v^{1/2}$) for NCM, NCMA, NCMA- CeO_{2-x} .

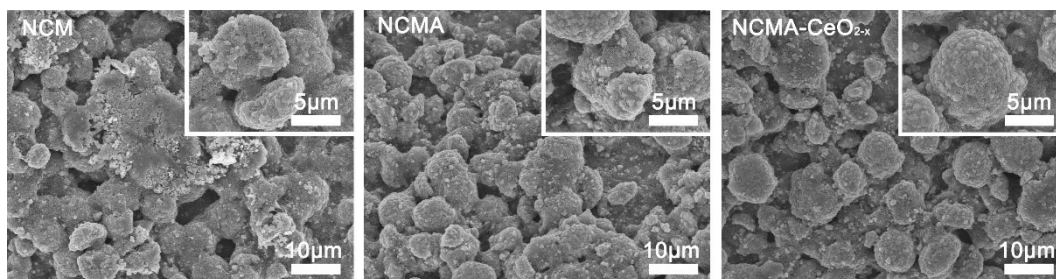


Figure S7 The SEM images of NCM, NCMA, NCMA- CeO_{2-x} after 100 cycles.

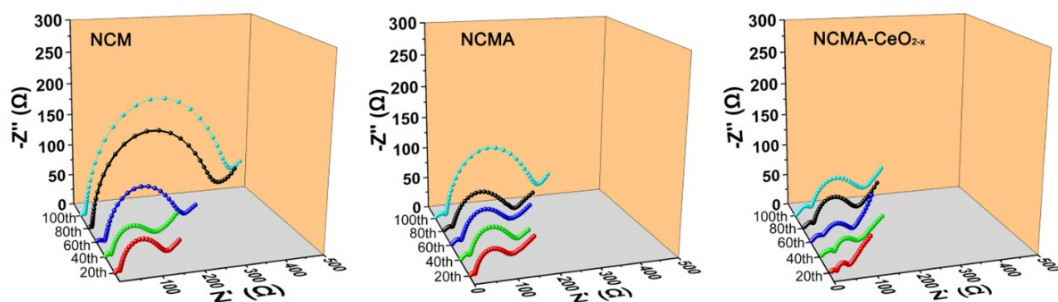


Figure S8 Nyquist plots after different cycles of NCM, NCMA, NCMA-CeO_{2-x}.

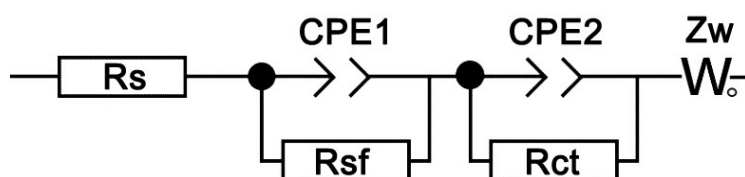


Figure S9 The equivalent circuit for the EIS test

The first semicircle in the high-medium frequency range is caused by surface film resistances (R_{sf}), while the second semicircle at the medium frequency is ascribed to the charge-transfer resistance (R_{ct}) of the cathode.

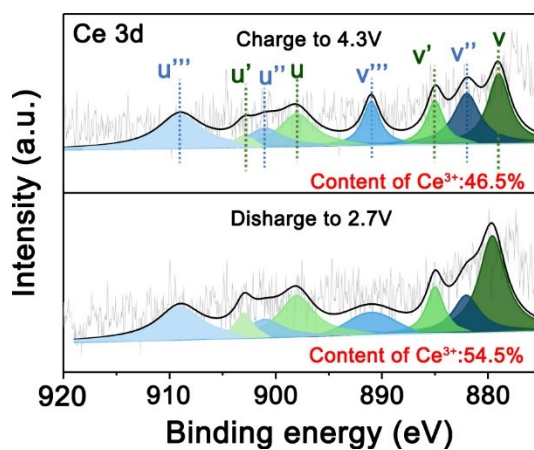


Figure S10 Ce 3d peaks of XPS spectra for NCMA-CeO_{2-x} at different potential.

Part 2 Supporting Tables

Table S1 Results of Rietveld refinements for NCM, NCMA, NCMA-CeO_{2-x}.

Lattice parameters				Ni/Li	wR _p	χ^2
a(Å)	c(Å)	c/a	V(Å ³)			

NCM	2.8702	14.198	4.946	101.292	3.89%	5.16%	0.8902
NCMA	2.8737	14.258	4.962	101.970	2.48%	4.56%	0.7332
NCMA-CeO _{2-x}	2.8735	14.254	4.961	101.927	2.52%	4.62%	0.7832

Table S2 Electrochemical performance of recent CeO₂ coating cathode materials reported in the literatures

Modified cathode material	Cutoff voltage (V)	Capacity at 0.1C (mAh g ⁻¹)	Capacity at 10C (mAh g ⁻¹)	Cycling (1C,100r)	Ref.
LiNi_{0.9}Co_{0.045}Mn_{0.045}Al_{0.01}O₂	2.7-4.4	222	140	96.7%	This work
Li _{1.2} Mn _{0.54} Ni _{0.13} Co _{0.13} O ₂	2.0-4.8	260	<100	86.9%	1
LiNi _{0.8} Co _{0.1} Mn _{0.1} O ₂	2.75-4.5	205	146	86.9%	2
LiNi _{0.9} Co _{0.05} Mn _{0.05} O ₂	2.8-4.3	215	125	93.3%	3
Li _{1.13} Ni _{0.2} Mn _{0.47} Co _{0.2} O ₂	2.0-4.8	220	<100	<80%	4
LiNi _{0.7} Co _{0.2} Mn _{0.1} O ₂	3.0-4.3	205	100	86.4%	5
LiNi _{0.5} Co _{0.2} Mn _{0.3} O ₂	2.7-4.6	195	120	74.5%	6

Reference

- [1] G. Hu, Z. Xue, Z. Luo, Z. Peng, Y. Cao, W. Wang, Y. Zeng, Y. Huang, Y. Tao, T. Li, Z. Zhang, K. Du, *Ceram. Int.*, 2019, **45**, 10633-10639.
- [2] F. Wu, Q. Li, L. Chen, Y. Lu, Y. Su, L. Bao, R. Chen, S. Chen, *ChemSusChem*, 2019, **12**, 935-943.
- [3] X. Zhang, G. Hu, K. Du, Z. Peng, W. Wang, C. Tan, Y. Wang, Y. Cao, *Ionics*, 2022. DOI: 10.1007/s11581-022-04832-9.
- [4] K. A. Kurilenko, O. A. Shlyakhtin, D. I. Petukhov, A. V. Garshev, R. G. Valeev, *J. Solid State Electr.*, 2019, **23**, 433-439.
- [5] S. Dong, Y. Zhou, C. Hai, J. Zeng, Y. Sun, Y. Shen, X. Li, X. Ren, G. Qi, X. Zhang, L. Ma, *Ceram. Int.*, 2019, **45**, 144-152.
- [6] H. Yi, L. Tan, L. Xia, L. Li, H. Li, Z. Liu, C. Wang, Z. Zhao, J. Duan, Z. Chen, *Adv. Powder Technol.*, 2021, **32**, 2493-2501.